Appl. Phys. B 62, 273–278 (1996)

Applied Physics B Lasers and Optics

Sensitive density-fluctuation measurements using wavelength-modulation spectroscopy with high-order-harmonic detection

A. N. Dharamsi*, Y. Lu

Department of Electrical and Computer Engineering, Old Dominion University, Norfolk, VA 23529-0246, USA
(Fax: + 1-804/683-3320, E-mail: AND100f@eefs01.ec.odu.edu)

Received: 4 April 1995/Accepted: 6 September 1995

Abstract. We discuss experimental and theoretical results which show that when wavelength-modulation spectroscopy is used to monitor concentration fluctuations of gaseous species, greater sensitivity may be obtained if one uses high-order detection. We also show that, depending on the ambient concentration being monitored, there are regions in which the commonly used second derivative would show a negligible variation of signal magnitude with concentration fluctuations, whereas measurement with a higher harmonic would result in a much improved signal. Theoretical results for the measurements of any transition that can be described by the Voigt profile are given. The technique discussed is illustrated by presenting the results of measurements of wavelength-modulation spectroscopy of lines in the oxygen *A* band. Different detection harmonic orders are suitable for different ambient concentrations, and a related criterion that helps in the determination of a suitable detection harmonic order is given.

PACS: 07.65; 42.60; 42.80

Wavelength-modulation spectroscopy has been used by many researchers [1–5] in the past to perform sensitive absorption measurements. Recent advances in diode laser technology have allowed the method to be applied in a wide range of environments, and it is expected that, with the development of diode lasers in the shorter-wavelength region of the visible spectrum, the number of applications of this technique will increase even more.

In addition to being easily tunable, diode lasers are particularly suitable for performing modulation spectroscopy, because the band gap and intensity are dependent on the injected current, making amplitude and frequency (wavelength) modulation particularly simple. When such wavelength-modulation spectroscopy is performed with small modulation indices, and detection is performed at a harmonic of the modulation frequency, derivative spectra are obtained. In particular, second-harmonic detection has been utilized quite extensively. While often the second-harmonic detection technique is quite adequate, there are instances in which the use of higher-order detection has advantages [6–8]. In this paper, we demonstrate experimentally how, when one performs higher-order-harmonic detection, the sensitivity with which fluctuations around an ambient density can be measured is increased. A theoretical treatment which describes the behavior of the signal expected, using any detection harmonic order, is given for any transition described by a Voigt function. Experimental results are given and compared to the ones predicted by theory.

1 Theoretical background

It can be shown [1, 2] that the signal (in W cm^{-2}) measured using Nth-harmonic detection, when the modulation index used is small, is given by

$$S_N = I_0 L \frac{2^{1-N}}{N!} a^N n \bar{\sigma} g^N(v). \tag{1}$$

Here, a is the frequency-modulation amplitude (in Hz), n (in cm^{-3}) is the absorber density, $\bar{\sigma}_{abs}$ is the length of the absorbing path (in cm), integrated absorption cross-section (in cm^2 Hz), and $g^N(v)$ (in Hz$^{-(N+1)}$ is the N-th derivative of the line shape function. (This expression needs to be modified when the modulation index is not small, and the correction terms are given in Sect. 1.1.)

1.1 Collision-broadened regime

If the line shape function is a Lorentzian (as in the collision-broadened regime, in which $\Delta v_{coll} = n\sigma_{coll} v$, where n is the density, σ_{coll} is the collision cross-section and v the relative velocity during molecular collisions), then it is

* To whom all correspondence should be addressed

relatively straightforward to show [7, 8] that with $(\nu - \nu_0)^2 + (\Delta\nu_{coll}/2)^2 = y$, the N-th derivative $\partial g_L^N/\partial\nu^N = g_L^N$ is given by

$$g_L^N = \left(\frac{\Delta\nu}{2\pi}\right)\frac{(-1)^N}{y^{N+1}}\sum_{k=0}^{[N]/2} C_{2k,N}\left(\frac{\Delta\nu}{2}\right)^{2k}(\nu-\nu_0)^{N-2k}, \quad (2)$$

where $[N] = N - 1$ if N is odd, and $[N] = N$ if N is even, and where

$$C_{2k,N} = (-1)^k\frac{(N+1)!}{2k+1}\binom{N}{2k}, \quad \text{with}\ \binom{N}{2k} = \frac{N!}{(2k)!\,(N-2k)!}. \quad (3)$$

It follows then that at line center, ν_0, the signal (when N is even) becomes

$$S_{NL}(\nu_0) = (-1)^{N/2} I_0 L 2^2 \frac{a^N}{\pi}\frac{\bar{\sigma}_{abs}}{(\sigma_{coll}\nu)^{N+1}}\frac{1}{n^N}. \quad (4)$$

(Note that for an odd derivative order, N, the signal at line center is zero, but the discussion may be extended to odd derivatives by calculating, for example, the magnitude of the signal at the first turning point. The subscript L denotes a Lorentzian line. Further, we have used the fact that the integrated absorption coefficient is $\bar{\alpha} = \bar{\sigma}_{abs}n$, where $\bar{\sigma}_{abs}$ is the integrated absorption cross-section.) Equation (4) shows that, in the collision-broadened regime, one expects the signal magnitude to vary as n^{-N}. (Strictly speaking, of course, the signal obtained on the detector will be proportional to the right-hand side of (4), because the latter does not account for the responsivity of the detector – for example in V W^{-1} cm^{-2}).

1.2 Doppler-broadened regime

Similarly, it can be shown [7, 8] that the Nth derivative, $g_G^N(\nu)$, of a Gaussian line can be written as

$$g_G^N(\nu) = \frac{g(\nu)}{\sqrt{\pi}}\frac{1}{(\overline{\Delta\nu}_D)^{2N+1}}\sum_{k=0}^{[N]/2} C_{2k,N}(\overline{\Delta\nu}_D)^{2k}(\nu-\nu_0)^{N-2k}, \quad (5)$$

where

$$C_{2k,N} = (-1)^k\frac{N!}{(N-2k)!}\frac{(-2)^{N-2k}}{k!} \quad \text{and}$$

$$[N] = \begin{cases} N-1 & \text{for } N \text{ odd}, \\ N & \text{for } N \text{ even} \end{cases}$$

and

$$g(\nu) = \exp\left(\frac{-(\nu-\nu_0)^2}{(\overline{\Delta\nu}_D)^2}\right).$$

Here, $\Delta\nu_D$ is the Doppler width given by

$$\Delta\nu_D = 2\left(\frac{2kT\ln 2}{Mc^2}\right)^{1/2}\nu_0,$$

and

$$\overline{\Delta\nu}_D = \frac{\Delta\nu_D}{\sqrt{4\ln 2}}.$$

Hence, for even N, the signal, measured at line center, ν_0, in the low-pressure Doppler-broadened region (once again assuming a small modulation index) is given by

$$S_{NG}(\nu_0) = (-1)^{N/2} I_0 L 2^{1-N} a^N \bar{\sigma}_{abs} n \frac{1}{\sqrt{\pi}}\frac{1}{\overline{\Delta\nu}_D^{N+1}}\frac{1}{(N/2)!}. \quad (6)$$

In the Doppler regime, the magnitude of the derivative signal, measured at line center, increases linearly with density, as might be expected.

1.3 Voigt regime

A more complete treatment of modulation spectroscopy should address lines that are given by the Voigt line shape function.

For a Voigt profile, one can show that [7]

$$\bar{g}_v^N(\nu_0) = 0 \quad \text{for } N \text{ odd} \quad (7a)$$

and

$$\bar{g}_v^N(\nu_0) = \frac{2}{(\overline{\Delta\nu}_D)^N}\left\{\sum_{k=0}^{([N]/2)-1} C_{2k,N}\left[\sum_{p=0}^{(N-2k-2)/2}(D_{N-2k,p}b^{2p}) + (-1)^{(N-2k)/2}\frac{\pi}{2}b^{N-2k-1}\exp(b^2)\operatorname{erfc}(b)\right] + C_{N,N}\frac{\pi}{2b}\exp(b^2)\operatorname{erfc}(b)\right\} \quad (7b)$$

for even N.

Here, the Voigt line shape function $g_v(\nu)$ is given [9] by (8), which is written for convenience in a normalized form, $\bar{g}_v(\nu)$:

$$\bar{g}_v(\nu) = \frac{g_v(\nu)}{(1/\pi^{3/2})(b^2/\delta\nu_0)} = \int_{-\infty}^{\infty}\frac{dy\,e^{-y^2}}{(x+y)^2+b^2}, \quad (8)$$

$$b = \frac{\Delta\nu_{coll}}{2\overline{\Delta\nu}_D} = \frac{\delta\nu_0}{\overline{\Delta\nu}_D} \quad (9)$$

and

$$x = \frac{\nu_0 - \nu}{\overline{\Delta\nu}_D}. \quad (10)$$

In the equation for the Nth derivative of the Voigt line shape function (7b),

$$C_{2k,N} = \frac{(-1)^k N!}{(N-2k)!}\frac{1}{2^k}\frac{1}{k!}2^{N-k} \quad (11)$$

and

$$D_{2q,i} = \frac{\sqrt{\pi}}{2}(-1)^i\frac{[2(q-1-i)]!}{4^{q-1-i}}\frac{1}{(q-1-i)!}. \quad (12)$$

Equation (7b) is derived from

$$\bar{g}_v(x) = \int_{-\infty}^{\infty}\frac{dy\,e^{-y^2}}{D} = \mathscr{L}[y^0], \quad (13)$$

where

$$D = (x+y)^2 + b^2 \quad (14)$$

and the operator $\mathscr{L}[y^m]$ is defined by

$$\mathscr{L}[y^m] = \int_{-\infty}^{\infty} \frac{dy\, e^{-y^2}}{D} y^m. \tag{15}$$

Hence, an alternative way to write (7b) is

$$\frac{\partial^N \bar{g}_v(x)}{\partial x^N} = \mathscr{L}_y \left\{ \sum_{k=0}^{[N]/2} C_{2k,N} y^{N-2k} \right\}. \tag{16}$$

The strength of the Nth derivative signal of a Voigt line, measured at line center $v = v_0$, can then be obtained by substituting (8) and (7b) into (1). The proofs of (2), (5) and (7) are relatively easily obtained in the following manner. For the Lorentzian and Gaussian profiles, the repeated derivatives are seen to form a recognizable pattern. Once this is found, a formal proof by induction follows. For the Voigt profile, a similar procedure is followed except that the pattern is discerned after a repeated integral, derived from (15), is evaluated. A formal proof by induction then gives (7a) and (7b) above [7, 8]. Note that while (2) and (5) are valid for all v, (7a) and (7b) apply at line center, $v = v_0$. Note also that (7b) should reduce to (5) and (2), respectively, when the latter two are evaluated at line center, in the limits that $b \to 0$ and $b \to \infty$, respectively. This is relatively straightforward to show [10].)

1.4 Corrections due to finite modulation index

Equation (1) is valid in the limit of small modulation indices; in other words, one would get pure derivatives of the line shape functions only for small modulation indices. In practice, however, one needs to use finite modulation indices and therefore has to account for correction terms that appear. It can be shown by following the approach of Myers and Putzer [2] that the corrected terms for a Voigt signal can be written as

$$S_{NV}^{C} = S_{NV}^{0} \left[1 + \sum_{\ell=1}^{\infty} (m)^{2\ell} \frac{N!}{2^{2\ell}\ell!(N+\ell)!} \times \left(\frac{\sum_{k=0}^{[N+2\ell]/2} C_{2k,N+2\ell} \mathscr{L}_y[y^{N+2\ell-2k}]}{\sum_{k=0}^{[N]/2} C_{2k,N} \mathscr{L}_y[y^{N-2k}]} \right) \right]. \tag{17}$$

Here, m is the modulation index, given by $m = a/\overline{\Delta v}_D$. Hence, for example, the signal with the first-order correction term included, in an experiment employing second-harmonic detection, can be obtained by using $\ell = 1$ in (17):

$$S_{2V}^{C} \simeq S_{2V}^{0} \left[1 + \frac{m^2}{12} \times \left(\frac{C_{0,4}\mathscr{L}_y[y^4] + C_{2,4}\mathscr{L}_y[y^2] + C_{4,4}\mathscr{L}_y[y^0]}{C_{0,2}\mathscr{L}_y[y^2] + C_{2,2}\mathscr{L}_y[y^0]} \right) \right]. \tag{18}$$

Similarly, the absorption signal (for a Voigt line shape function) with corrections up to second order is given by using $\ell = 2$ in (17), and so on. Note that (17) can be evaluated explicitly since the correction terms are weighted higher pure derivatives, and these latter terms can be obtained by using 7(b).

2 Sample numerical results

The results of some computations for signals at line center for second-, fourth- and sixth-harmonic detection using (7b), (17) and (1) are shown in Fig. 1. [It is clear from (17)

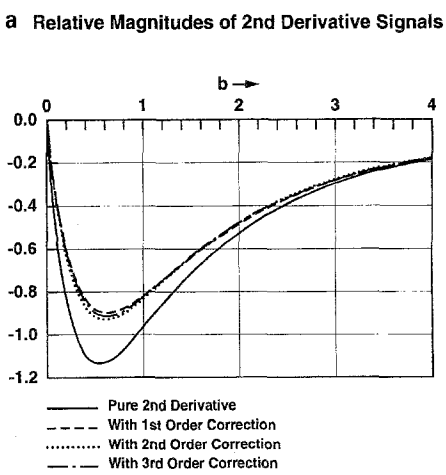

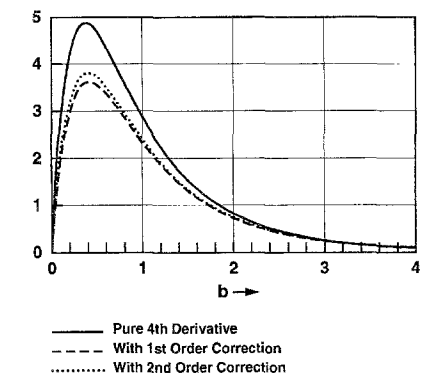

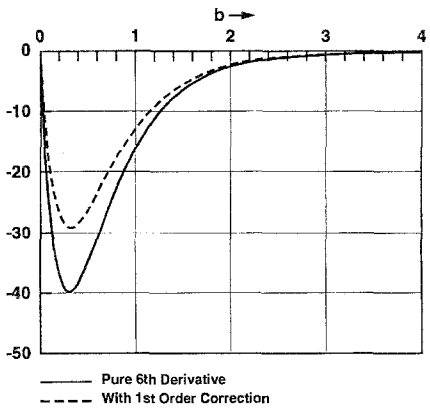

Fig. 1a–c. Computed signal magnitudes, for Voigt line shape functions, at the line center for second-, fourth- and sixth-harmonic detection; signals corrected for finite modulation index distortions ($m = 0.8$). Note the vertical scale is in units of $(I_0 L\bar{\sigma}/\pi^{3/2})(2/\sigma_{coll}v)(2^{1-N}/N!)m^N$. (**a**) Second-harmonic detection with corrections up to third order. (**b**) Fourth-harmonic detection with correction terms up to second order. (**c**) Sixth-harmonic detection with correction term up to first order

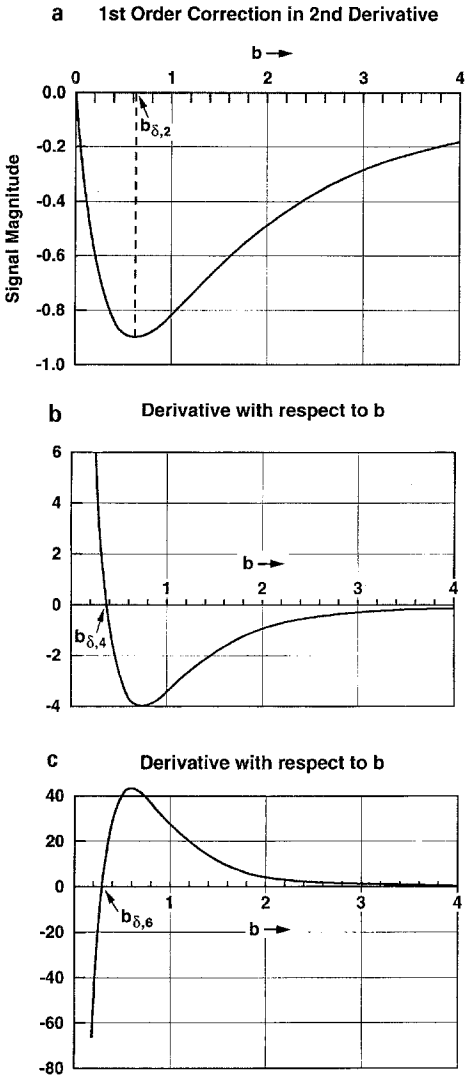

Fig. 2a–c. Computed sensitivities, of signal magnitudes at line center to density fluctuations; derivatives of signal magnitudes with respect to the parameter b. The vertical scale is in units of $(I_0 L\bar{\sigma}/\pi^{3/2})(2/\sigma_{\text{coll}}v)\,(2^{1-N}/N!)\,m^N$; (**a**) Second-harmonic detection; (**b**) fourth-harmonic detection; (**c**) sixth-harmonic detection

that the signal corrected for finite modulation index, m, must depend on the latter. In Fig. 1, we have used a value of $m = 0.8$.] These results have been computed using the Voigt line shape function. Note also that the signals are plotted as a function of the parameter b, given by (9); for the conditions of our experiment, namely a fixed temperature, b is directly proportional to the density n, since $\Delta\nu_{\text{coll}} = n\sigma_{\text{coll}}v$. It is seen from these figures that the behavior of the signal is as predicted by (4) and (6), being directly proportional to density in the Gaussian regime, and falling as n^{-N} in the collision-broadened region. Note that we have denoted the turning points of the signal (plotted against b) as $b_{\delta,N}$. Defining $n_{\delta,N} = b_{\delta,N}/\sigma_{\text{coll}}v$, it follows that the sensitivity of measurement of a density fluctuation around $n_{\delta,N}$, using Nth-harmonic detection, will be small. On the other hand, if the detection harmonic is changed then the sensitivity will be increased. (Clearly, this only applies over a certain range of N values, because other experimental effects would come into play that could result in a deterioration of the signal-to-noise ratio as N is increased.) This is shown in Fig. 2, which shows the derivative of the signal measured *with respect to b, and hence the density n* for $N = 2$, 4 and 6. Moreover, by definition of $b_{\delta,2}$, the derivative of the second-harmonic signal with respect to b is zero at $b_{\delta,2}$, the derivatives of the fourth- and sixth-harmonic signals are non-zero at $b_{\delta,2}$, and vice versa.

Table 1. Computed variation of $b_{\delta,N}$ with modulation index

Modulation index m	$b_{\delta,2}$, corrected to second order	$b_{\delta,4}$, corrected to second order	$b_{\delta,6}$, corrected to first order
0.1	0.552	0.374	0.300
0.2	0.555	0.375	0.301
0.3	0.560	0.376	0.302
0.4	0.565	0.378	0.303
0.5	0.575	0.382	0.306
0.6	0.582	0.387	0.309
0.7	0.595	0.392	0.313
0.8	0.608	0.395	0.320
0.9	0.620	0.402	0.328
0.99	0.632	0.406	0.340

It is seen by using (17) that when corrections for a finite modulation index are included, the values of $b_{\delta,N}$ and $n_{\delta,N}$ change somewhat. We have computed these values for modulation indices up to 0.99 and assuming a Voigt line shape function. Table 1 shows the values of $b_{\delta,N}$ that would be obtained if one incorporates corrections due to a finite value of m, the modulation index. From (17), it is seen that in order to obtain corrections up to second order for Nth-harmonic detection, one needs to evaluate $\bar{g}_v^N$ for $N = N$, $N + 2$ and $N + 4$. Hence, the second-order corrections in $b_{\delta,2}$ and $b_{\delta,4}$ require a computation of $\bar{g}_v^6$ and $\bar{g}_v^8$ respectively; the first-order corrections to $b_{\delta,6}$ require the computation of $\bar{g}_v^8$. The uncorrected values for $b_{\delta,2}$, $b_{\delta,4}$ and $b_{\delta,6}$ are $b_{\delta,2} = 0.550$, $b_{\delta,4} = 0.370$ and $b_{\delta,6} = 0.300$. Hence, it is seen that the density at which the signal at line center peaks, for a given order of harmonic detection, varies with m. It should be pointed out that the discussion given above regarding the sensitivities to density fluctuations remains unchanged because the values of $b_{\delta,N}$ for different values of N all increase monotonically with the wavelength modulation index, m.

3 Experimental results

Experimental measurements of the oxygen A band (the rotational lines in the $0 \leftarrow 0$ vibrational rung of the $b^1\Sigma_g^+ \leftarrow X^3\Sigma_g^-$ low-lying electronic transition) RR (15, 15) line, at various derivative orders, were taken by using an apparatus that has been described previously [6]. Figure 3 shows the results for pure O_2. The results are given in a normalized form, such a formulation being more illustrative when one considers percentage changes. The normalization is done so that the peak values of all the curves correspond to unity. (In practice, the magnitudes of the curves have to be multiplied by $(2^{1-N}m^N)/N!$.) One sees that the predictions of the theory above are borne out experimentally. For example, Fig. 3 shows that

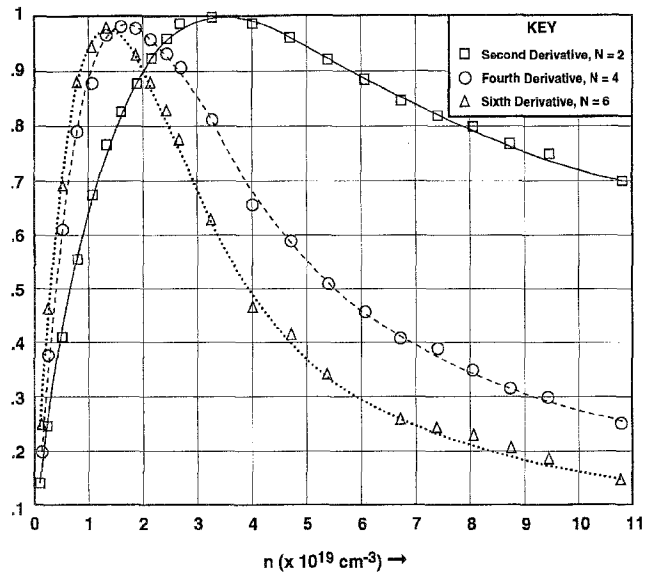

Fig. 3. Signal magnitudes at RR (15, 15) line center vs O_2 concentration for second-, fourth- and sixth harmonic detection. For convenience, all the signals have been normalized so that the peaks correspond to unity. The effective normalization factor is $(2^{1-N}/N!)m^N$

the variation of the signal, with respect to density in the collision-dominated region, is higher for higher derivatives (the factor $1/n^N$ in (1).) [It should be pointed out that in Fig. 3 we are displaying only the magnitudes of the signals – from (4), (6) and (7b), the sign of the signal is given by $(-1)^{N/2}$, as is depicted in Figs. 1a–c.]

The above experimental results show that the sensitivity of derivative absorption spectroscopy in the collision-broadened regimes can be increased, over given ranges of n, by increasing N. This is illustrated further in the experimental results shown in Fig. 4, which shows the absorption signal due to the RQ (13, 14) oxygen line (this line is centered at 13153.4219 cm^{-1} and has a strength of 5.521×10^{-24} cm^2 $molecule^{-1}$ cm^{-1} [11]) in air, at various concentrations of O_2 measured in the second and sixth derivatives. In this measurement, air was evacuated from and pumped into the chamber in order to ensure that the relative densities of the constituents were constant. (The concentration of oxygen is $0.21 \times 2.7 \times 10^{19}$ cm^{-3} at the zero of the horizontal scale, it is $0.22 \times 2.7 \times 10^{19}$ cm^{-3} at $\Delta n = 1\%$, it is $0.20 \times 2.7 \times 10^{19}$ cm^{-3} at $\Delta n = -1\%$, etc. Such measurements are of interest in several applications, for example in monitoring and optimizing the performance of combustion-driven wind tunnels, by varying the relative concentrations of the fuel). It is clearly seen that the slope of the sixth derivative signal is larger than that of the second derivative signal.

Small concentration variations around an ambient value can be measured from the magnitude of the signal by using higher detection harmonic order even when the concentration is such that one would not obtain any changes in the magnitude of the signal at lower orders. The experimental results shown in Fig. 4 illustrate this. These results show that the second-derivative (harmonic) signal magnitude exhibits a low sensitivity with respect to the density changes around the operating pressure under consideration (because one happens to be at a concentration close to $n_{\delta,2}$ – i.e. the value of the density where the second-derivative (harmonic) signal is stationary with respect to density fluctuations), whereas the sixth-harmonic signal is highly sensitive to concentration changes in this range.

4 Discussion

We have shown that when wavelength-modulation spectroscopy is used, the signal increases linearly with densities, peaking at densities given by $n_{\delta,N} = b_{\delta,N}/\sigma_{\text{coll}}v$, after

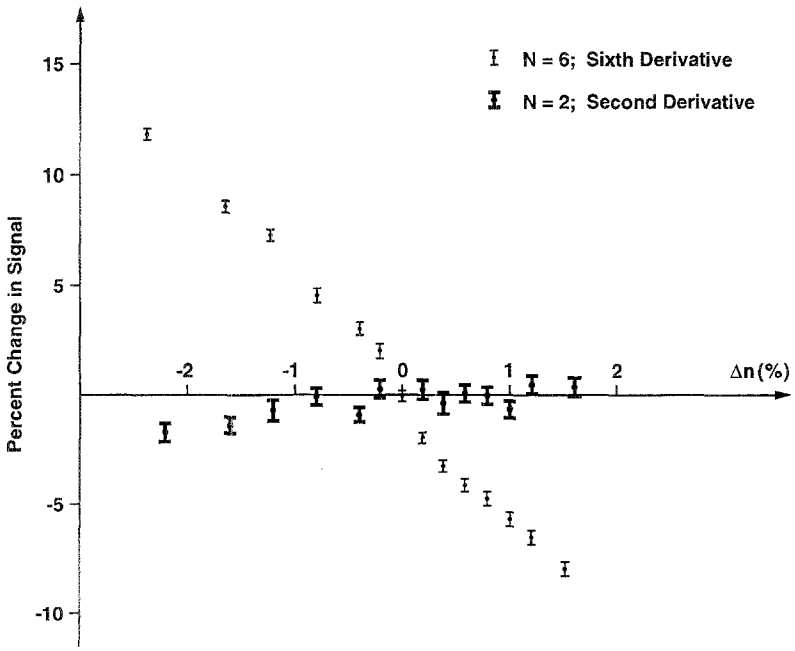

Fig. 4. Percentage change in signal magnitude at line center vs percentage change in oxygen concentration, around $n_{\delta,2}$ (air was used in the chamber, and the relative concentrations of constituents were fixed)

which the signal magnitude falls approximately as n^{-N}. The densities $n_{\delta,N}$ serve to delineate the effective Doppler regime from the effective collision-broadened regime, and these densities can be evaluated for detection with any order harmonic (Table 1).

This behavior of the measured signal allows one to obtain greater sensitivities in measurements of density fluctuations when using higher-harmonic detection. It is also seen that when monitoring density fluctuations, by measuring the magnitude of the signal at line center, around $n_{\delta,N}$, one should avoid using Nth-harmonic detection. For example, one would want to avoid using second-harmonic detection to monitor fluctuations of density around $n_{\delta,2}$; at these densities, one would want to use higher-harmonic detection. Extending this discussion, it is seen that, *in order to measure the variations of density around concentrations corresponding to* $n_{\delta,N}$, *one should use a detection harmonic other than* N.

Since the sensitivity of a detection technique depends on the signal-to-noise ratio and not just the signal itself, the ultimate choice of N will depend on aspects such as the noise environment in the particular experiment, and the dynamic range of the phase-sensitive measurement apparatus. As one goes to higher-harmonic detection, the bandwidth required by the phase-sensitive electronic detection system increases. One also has to ensure that the overall noise at this frequency does not negate any advantage that would otherwise be obtained. In practice, the latter is relatively easily satisfied in the case where the modulation frequency is relatively low and, in fact, in many situations where $1/f$ noise dominates, one would actually obtain a reduction in the noise and, hence, an increase in the signal-to-noise ratio just by operating in the higher-frequency domain. Nonetheless, ultimately, the most suitable order would have to be determined experimentally. The results of the present work, however, show that one could use a diode laser sensor to measure fluctuations of concentrations, in a large range of practical interest, if one chooses the detection harmonic order carefully.

Acknowledgements. It is a pleasure to acknowledge helpful discussions with Professor Adil Hassam and Dr. Yozo Mikata. The assistance of Mr. I. Stouklov with experiments is also acknowledged.

References

1. J. Reid, D. Labrie: Appl. Phys. B **26**, 203 (1981)
2. O.E. Meyers, E.J. Putzer: J. Appl. Phys. **30**, 1987 (1965)
3. R. Arndt: J. Appl. Phys. **36**, 2522 (1965)
4. G.V.H. Wilson: J. Appl. Phys. **34**, 3276 (1963)
5. D.T. Cassidy, J. Reid: Appl. Phys. B **29**, 279 (1982)
6. A.D. Jackson, A.N. Dharamsi, S.K. Chaturvedi: In *Laser Applications to Chemical Analysis*, 1994 Tech. Dig. Ser., Vol. 5 (Optical Society of America, Washington, DC 1994) pp. 43–46
7. A.N. Dharamsi, A.D. Jackson, Y. Lu: *IEEE Lasers and Electro-Optics Society Meeting, LEOS'94*, 7th Annual Meeting,. Boston, MA (October 1994) Paper SL1.2
8. A.N. Dharamsi, Y. Lu: Appl. Phys. Lett. **65**, 2257 (1994)
9. P.W. Milloni, J.H. Eberly: *Lasers* (Wiley-Interscience, New York 1988)
10. A.N. Dharamsi, Y. Lu: Unpublished
11. L.S. Rothman, R.R. Gamache, A. Goldman, L.R. Brown, R.A. Toth, H.M. Pickett, R.L. Poynter, J.M. Flaud, C. Camy-Peyret, A. Barbe, N. Husson, M.A.H. Smith: Appl. Opt. **26**, 4058 (1987)